臨床応用を行っている（表１）。人工材料を用いた再生医療を応用するにあたり、患者・家族には治療内容を十分に説明し同意を得た上で、京都大学付属病院および福島県立医科大学付属病院において本再生治療を実施している。

以下にこれまでの臨床応用例の概略を記載する。

①症例１：甲状腺進行癌の気管浸潤例

79歳女性、主訴は右頸部腫脹。CTにて、甲状腺右葉全体を占める直径約５cmの腫瘍を認め、頸部気管右側への浸潤が疑われ、気管内視鏡でも声門下に続く気管内腔の右側に隆起を認め、甲状腺腫瘍の気管浸潤と考えられた（図１）。

手術は、全身麻酔下に頸部襟状切開を加え、甲状腺腫瘍を露出した。甲状腺右葉は腫瘍で占拠され、頸部気管に癒着していた。癌組織の浸潤した頸部気管を、安全域を付けて３気管輪、半周を切除した（図２）。その欠損部に本人工材料をトリミングして２/３周分の材料に自己の血液を注射器で注入し、気管欠損部をパッチする形で縫合した。

術後の気管内視鏡所見を図３に示す。術後２週間にはコラーゲンとメッシュが透見され、術後２カ月で上皮化し人工材料はほぼ被覆され、術後４年２カ月の時点では、気管内腔面は上皮で覆われ組織再生は良好な経過である。

②症例２：甲状腺進行癌気管浸潤例

71歳男性。主訴は前頸部腫脹。CTにて、甲状腺右葉に腫瘍を認め、甲状腺癌気管浸潤が疑われた。

手術は全身麻酔下にて行い、甲状腺腫瘍を露出した。腫瘍は右反回神経を巻き込んでおり、神経切断を余儀なくされた。腫瘍は第１－２気管輪に浸潤しており、約半１/３周切断した。その欠損部は10㎜×12㎜で、本人工材料をトリミングして１/２周分の材料に自己の血液を注射器で注入し、気管欠損部をパッチする形で縫合した。術後３日目に軽度のair leakを認めたが、ドレインと圧迫で軽快した。術後３年１ヵ月経過した現在、気管内腔の上皮化は良好で順調な経過である。

③症例３：甲状腺癌再発気管浸潤例

59歳女性。S63年に他施設にて甲状腺癌の診断にて甲状腺左葉切除術を施行され、H13に局所再発し左上極気管浸潤にて甲状腺全摘術を行った上で^{131}－Ｉ内照射を施行された。H16年に局所再発、CTにて腫瘍は輪状軟骨、気管に浸潤が認められた（図４）。

手術は全身麻酔下にて行い、残存した前頸筋を剥離していくと甲状軟骨、輪状軟骨が現れた。輪状軟骨の一部が破壊され、第１－２気管軟骨も破壊されており、腫瘍が露出していた。左反回神経は腫瘍を貫いており、切断を余儀なくされた。腫瘍を剥離し、基部を含む輪状軟骨下縁、第１－２気管輪を半周切断した。その欠損部に本人工材料をトリミングして２/３周分の材料に自己の血液を注射器で注入し、気管欠損部をパッチする形で縫合した（図５）。

術後２週間ではコラーゲンメッシュの露出がみられていたが、術後２ヵ月で人工材料内腔面ほぼ上皮化し、術後２年１ヵ月の時点で、気管内腔面は上皮で覆われ組織再生は良好な経過である（図６）。３－DCTにて術前と術後を比較し人工材料の被覆状況が確認できた（図７）。

１．喉頭気管狭窄

①症例４：喉頭気管狭窄症

73歳男性。主訴は呼吸困難。喉頭ファイバーで声門下に肉芽、瘢痕の増生を認め気管内腔の径が約５㎜に狭小化し（図８）、CTでは気管内腔の90％狭小化を認めた。手術は局所麻酔下に気管切開を行った。後日創部感染がないことを確認した上で全身麻酔下に狭窄組織除去術を行い、甲状軟骨下縁及び輪状軟骨の一部を肉芽とともに合併切除した。最終欠損径は15㎜×７㎜であった（図９）。本人工材料を25㎜×17㎜にトリミングしたものに自己の血液を浸透させパッチする形で縫合固定した（図10）。

術後の気管内視鏡所見を図７に示す。術後２週間ではコラーゲンメッシュの一部露出が認められ、術後２ヵ月で人工材料に一致して肉芽造成がみられたが自然消退し最終的には上皮化し人工材料はほぼ被覆され、術後９ヵ月の時点では気管内腔面は上皮で覆われ組織再生は良好な経過である（図11）。3-DCTにて術前と術後を比較し人工材料の被覆状況が確認できた（図12）。

②症例５：気管狭窄症

42歳、女性。主訴は呼吸困難。他施設にて特発性気管狭窄症に対して手術を受けたが、再狭窄をきたしたため、再度喉頭截開を受け、Ｔチューブ挿入となった。CT上、輪状軟骨と第１－３気管輪レベルで内腔の狭小化を認めた（図13）。

手術は、先に全身麻酔下に声門下瘢痕除去、右頬粘膜移植を行い、Ｔチューブ抜去後も再狭窄が起きないことを確認した。後日、全身麻酔下に瘻孔部の皮膚と内腔の肉芽を気管軟骨とともに切除し、最終的な軟骨欠損部は15×５㎜であった。その欠損部に本人工材料を25×24㎜にトリミングしパッチする形で縫合した（図14）。

喉頭内視鏡所見として、術後２週間ではコラーゲンメッシュの一部露出と白苔の付着がみられていたが、術後２ヵ月で人工材料内腔面はほぼ上皮化し、術後12ヵ月の現時点で、気管内腔面は上皮で覆われ再狭窄も認めず組織再生は良好な経過である（図15）。術後CTでは、気管軟骨欠損部を被覆する人工材料が確認され、内腔の再狭窄や気腫などの合併症も認めていない（図16）。

③症例６：喉頭気管狭窄症

29歳女性。主訴は呼吸困難。平成15年12月に飲酒後転倒した際、ガラスに頭から突っ込んでしまい、頸部切傷受傷。他施設にて緊急手術となり気管切開のうえ喉頭閉鎖術を施行し、以降レティナ管理となった。当科受診時、喉頭所見では声帯にweb形成がみられ声門の１/２は狭窄し固定していたが、両披裂部の可動性は比較的良好であった。CTでは甲状軟骨前方が声帯レベルから声門下にかけて欠損していた。声門下には厚い瘢痕組織を認めた。

手術は、先に全身麻酔下に喉頭截開による声門形成術を施行しweb切除を行った。その後web再形成が無いことを確認した上で、全身麻酔下に前頸部の瘢痕と瘻孔の周囲に皮膚切開をおき瘢痕除去から行った。瘢痕を鋭的に切離し最終的な甲状軟骨欠損部位の大きさは内周が15×7㎜、外周が20×17㎜であった。その欠損部に本人工材料を30×25㎜にトリミングして自己の血液を注入し、気管欠損部をパッチする形で縫合した。

術後2週間ではコラーゲンメッシュの一部露出が認められ、術後2ヵ月で人工材料に一致して肉芽造成がみられたが自然消退し最終的には上皮化し人工材料はほぼ被覆され、術後1年2ヵ月の現時点では気管内腔面は上皮で覆われ組織再生は良好な経過である。

④症例7：特発性気管狭窄症

29歳、女性。主訴は呼吸困難。平成3年に意識消失発作にて某大学病院小児科を受診し、てんかん等が疑われたが原因不明であった。平成7年呼吸苦出現し同院耳鼻咽喉科初診、頚部Xp、内視鏡で全周性の声門下狭窄と診断された。平成8年と9年に合計4回の喉頭気管形成術をうけたが再狭窄を来し、T-tubeを輪状軟骨から第1、2気管軟骨の高さに挿入した。

手術は、全身麻酔下に瘻孔部の皮膚と内腔の肉芽を除去し、最終的な軟骨欠損部は11×20㎜に形成した。同部に末梢血で湿潤した組織再生型人工材料を22×35㎜にトリミングしパッチする形で縫合した。

術後2週間では白苔の付着がみられていた。術後1ヵ月程で軽度肉芽形成を認めたが、術後3ヵ月では人工材料内腔面はほぼ上皮化し、現在のところ再狭窄も認めず組織再生は良好な経過である。

D．考　察

気道に悪性腫瘍が浸潤した例や気道の炎症性疾患、気道の狭窄、外傷例などで病変を切除した際、気道欠損部の再建が問題になる。これには、気道としての硬度を持った枠組みと内腔粘膜を同時に再建する必要がある。従来、硬性組織には各種の軟骨、骨、人工材料などが、内腔面組織には皮膚や粘膜などが用いられたが、二期的にしかも他部位の手術が必要である。また、気管切除後の端々吻合術は、縫合不全の可能性や術後の挿管および頸部前屈体位など解決すべき問題点が残されている。

1960年代から人工気管については多くの研究が行われてきたが、現在まで安心して臨床使用できる人工材料は開発されていない。Nevilleらの人工気管が一時的に臨床応用されたが、気管断端との接合部の離開が起こり現在は使われていない。中村らは1985年頃より様々な人工気管を試作してきたが、1995年、自己組織が再生するようにデザインした人工材料を開発し、動物実験で良好な気管再生を実現できることを報告した。同様の人工材料を輪状軟骨の切除後の欠損モデルに移植し、再生組織は正常と同等の硬さを持ち、かつ良好な上皮化が得られることがわかった。

臓器再生には足場、細胞、環境調節因子が必要で、この三要素に加えて血流が供給されると臓器再生が得られるとされている。本研究では足場のみの移植を行い、組織再生をはかった。

組織工学（tissue engineering）は、工学的手法を使って細胞を二次元的、三次元的に組み上げ、本物の臓器や組織に近いものを再生させようというもので、Vacanti、Langerらによって始められた。彼らのtissue engineeringは、体外で細胞を培養して目的とする組織をつくり、これを体内に移植する方法である。この考え方でKojimaらは羊の鼻中隔軟骨と上皮細胞を培養し、シリコンチューブの周囲に内腔を上皮に被覆された軟骨管を作製しマウスの背中に移植した。これにより正常の気管とよく似た管腔組織を再生させたが、ヒトへの臨床応用には超えなければならないハードルがある。

幹細胞や前駆細胞を移植することで組織再生をはかろうという研究が数多く行われている。自己由来の細胞移植としては、循環器領域で下肢や心筋の血管再生を目指した血管内皮前駆細胞の移植、整形外科領域で骨関節疾患の治療に骨髄間葉系幹細胞の移植、眼科領域で角膜再生を目指して角膜上皮幹細胞を羊膜上で培養した移植などある。

一方、我々の研究グループでは、体内の、再生を目的とする臓器の場所で組織を再生させる*in situ* Tissue Engineeringという新しい概念に基づいて、1997年以後、動物実験で自己組織再生型の人工材料を移植し気管、食道、胃、輪状軟骨などが再生することを報告してきた。これらの実験では細胞移植や増殖因子は使わずに足場の移植のみでの組織再生を行ってきた。Vacantiらのように体外で組織を再生してから移植する方法や、自己由来であっても細胞移植を行うと、生きた細胞や組織を取り扱うので、感染症対策や細胞の品質管理など臨床応用へのハードルが高い。これらの方法に比べて、我々の行っている*in situ* Tissue Engineeringにより足場のみを移植する手法は安全性が高く臨床応用に近いといえる。気管、輪状軟骨までは、この方法である程度満足する成績が得られるものと思われる。

臨床応用の経過から被覆した人工材料内腔面の上皮化には最低でも2カ月を要することが判ってきた。さらに喉頭レベルの症例では一旦肉芽形成がみられ、その消退に伴い上皮化が起こる傾向にあることも判った。上皮化の遅延は創部感染を惹起する危険性があり、次のステップとして解決すべき問題点は、上皮化を加速する方法の開発であり、さらには形態の複雑な喉頭、特に声帯の再生などがあげられる。これらの臨床的問題点をフィードバックさせ、本研究グループでは気道の上皮再生を加速するために、気管上皮細胞の培養、気管上皮細胞と人工材料からなるハイブリッド型の足場材料を開発し、その細胞の性質を免疫組織化学的手法で解析している。また、声帯の隆起を再生するために、喉頭内腔を型どりした材料を作製した。これらの結果は別項目に述べたが、問題点を克服することで、より多くの患者により安定した喉頭・気管の再生治療を実現できると考えられる。

E．結　論

われわれは、体内で自己組織の再生を誘導する *in situ* Tissue Engineering の考え方で気道再生研究を行った。ポリプロピレンメッシュとコラーゲンスポンジから構成される足場材料を開発し、動物実験で気道の安定した組織再生が得られた。これらの結果をふまえて世界に先駆けて頸部気管で臨床応用を開始し全例において現時点では気管内腔は上皮化し順調である。しかしながら、現時点で上皮化は早期には得られておらず、今後も更なる工夫が必要であると考える。気道の再生治療は端緒についたばかりであり、今後臨床成績を長期的に評価することが重要である。

F．研究発表

1．論文発表

1）Kobayashi K, Nomoto Y, Suzuki T, Tada Y, Miyake M, Hazama A, Kanemaru S, Nakamura T and Omori K. Effect of fibroblasts on tracheal epithelial regeneration in vitro. Tissue engineering 12, 2619-2628, 2006

2）Nomoto Y, Suzuki T, Tada Y, Kobayashi K, Miyake M, Hazama A, Wada I, Kanemaru S, Nakamura T, Omori K: Tissue Engineering for regeneration of the tracheal epithelium. Ann Otol Rhinol Laryngol. 115: 501-6, 2006

3）大森孝一，中村達雄，多田靖宏，野本幸男，鈴木輝久，小林　謙，佐藤　聡，金丸眞一，安里　亮，山下　勝：気管の再生と臨床応用，分子呼吸器病，第10巻，216－219，2006

4）大森孝一，中村達雄，多田靖宏，野本幸男，鈴木輝久，金丸眞一，安里　亮，山下　勝：甲状腺癌治療における気道の再生医療．再生医療．5：89－93, 2006

5）大森孝一，多田靖宏，松塚　崇，野本幸男，鈴木輝久，中村達雄，金丸眞一，安里　亮，山下　勝，田中信三：喉頭・気管狭窄の再生治療．日本気管食道科学会会報．57：153－154, 2006

2．学会発表

1）Omori K, Tada Y, Suzuki, T, Nomoto Y, Nakamura T, Kanemaru S, Yamashita M, Asato R:Clinical application of in situ tissue engineering for the laryngeal and tracheal tissue.127th American Laryngological Association (2006.5. 19-20 Chicago)

2）Nomoto Y, Kobayashi K, Suzuki T, Tada Y, Miyake M, Omori K, Hazama A, Nakamura T: The effects of fibroblasts upon the epithelial regeneration on the surface of the artificial trachea. 86th The American Broncho- Esophagological Association (2006.5.19-20 Chicago)

3）多田靖宏，野本幸男，鈴木輝久，小林　謙，金丸眞一，大森孝一：組織工学的手法を用いた気道再生の臨床応用，第58回日本気管食道科学会学術講演会（2006.10.5-6，札幌）

4）野本幸男，小林　謙，多田靖宏，鈴木輝久，三宅将生，挾間章博，和田郁夫，中村達雄，大森孝一：上皮細胞層を有するハイブリッド型人工気管の作製，第107回日本耳鼻咽喉科学会総会（2006．5．11，東京）

5）野本幸男，鈴木輝久，多田靖宏，小林　謙，三宅将生，挾間章博，中村達雄，大森孝一：上皮細胞層を有するハイブリッド型人工気管の作製．第107回日本耳鼻咽喉科学会総会（2006.5.11-13，東京）

6）野本幸男，鈴木輝久，多田靖宏，小林　謙，三宅将生，狭間章博，和田郁夫，中村達雄，金丸眞一，大森孝一：上皮細胞層を有するハイブリッド人工気管作製の試み．第27回日本炎症・再生医学会（2006.7.11-12，東京）

7）野本幸男，小林　謙，多田靖宏，佐藤　聡，岡野　渉，和田郁夫，中村達雄，大森孝一：線維芽細胞を組み合わせたハイブリッド人工気管作製の試み．第９回日本組織工学会（2006.9.7-8，京都）

8）野本幸男，小林　謙，多田靖宏，鈴木輝久，佐藤　聡，和田郁夫，金丸眞一，中村達雄，大森孝一：気管由来線維芽細胞を含有したハイブリッド人工気管モデル．第58回日本気管食道科学会（2006.10.5-6，札幌）

G．知的財産権の出願・登録状況

1．特許取得

なし

2．実用新案登録

なし

3．その他

なし

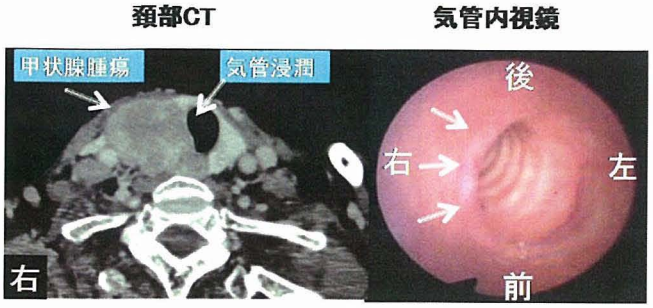

図１．症例１：術前所見

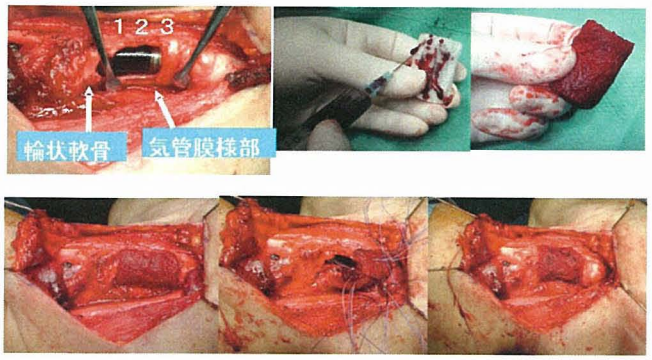

図２．症例１：術中所見

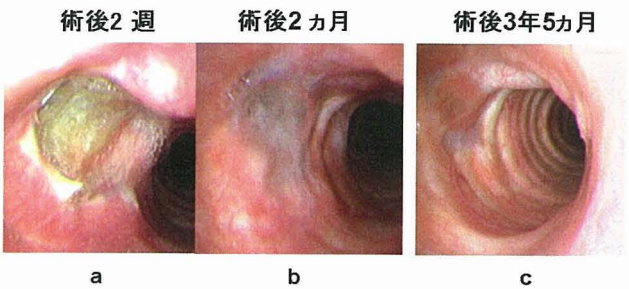

図３．症例１：術後喉頭ファイバー所見
ａ：人工材料の上皮化は不十分
ｂ：ほぼ上皮化
ｃ：全て上皮化

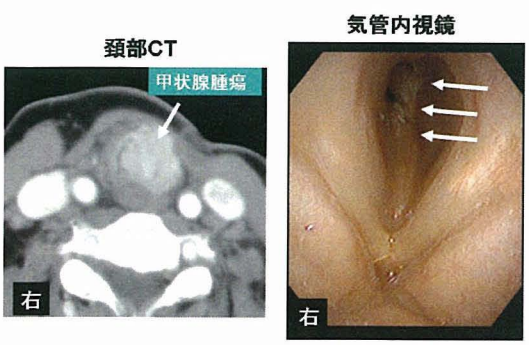

図４．症例３：術前所見

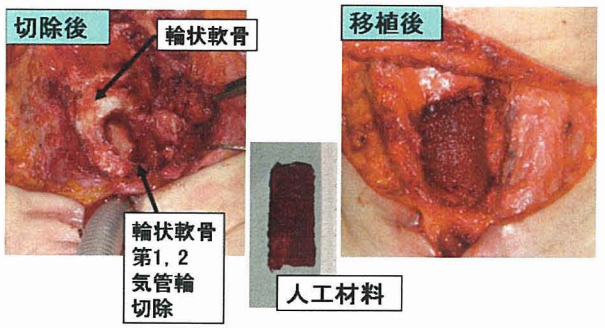

図５．症例３：術中所見

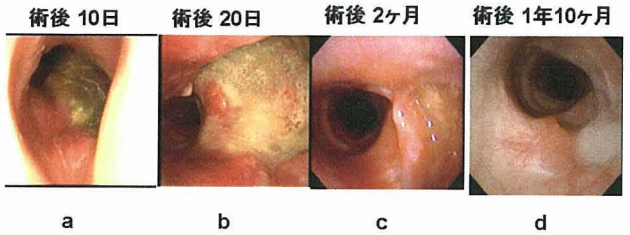

図６．症例３：術後ファイバー所見
ａ：人工材料露出あり
ｂ：一部上皮化あり
ｃ：ほぼ上皮化
ｄ：完全上皮化

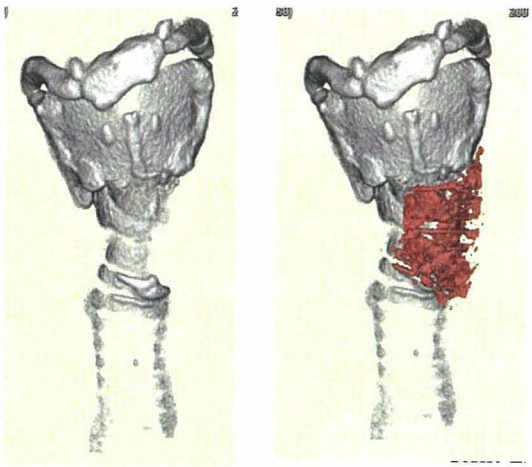

図７．症例３：3DCT
ａ：術前
ｂ：術後（赤色部分は人工材料）

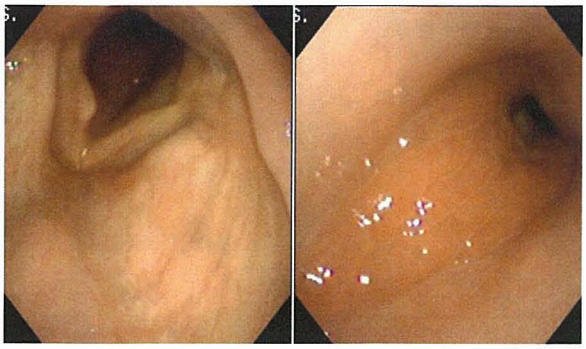

a　　b

図８．症例４：喉頭ファイバー所見
ａ：声門腔
ｂ：声門下腔（内腔の90％狭窄）

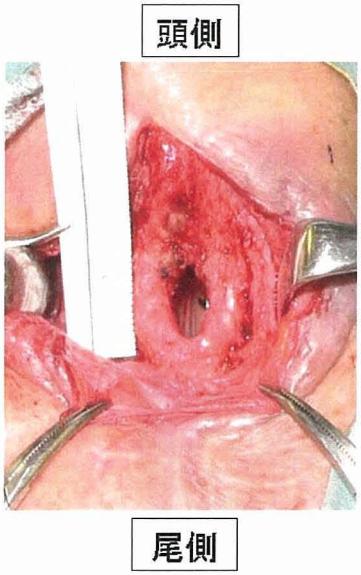

図９．症例４：欠損部（15×７㎜）
甲状軟骨下縁の一部から第３気管輪までの欠損

図10．症例４：人工材料被覆（25×17㎜）

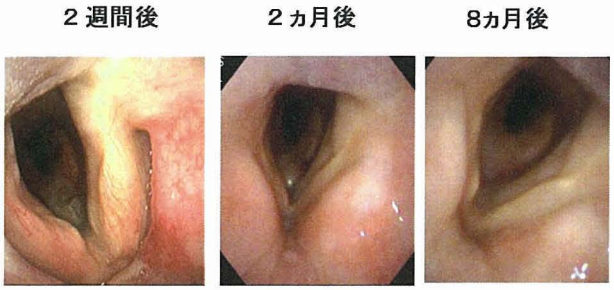

図11．症例４：術後喉頭ファイバー所見
ａ：人工材料の上皮化不十分
ｂ：人工材料上に肉芽形成
ｃ：上皮化あり

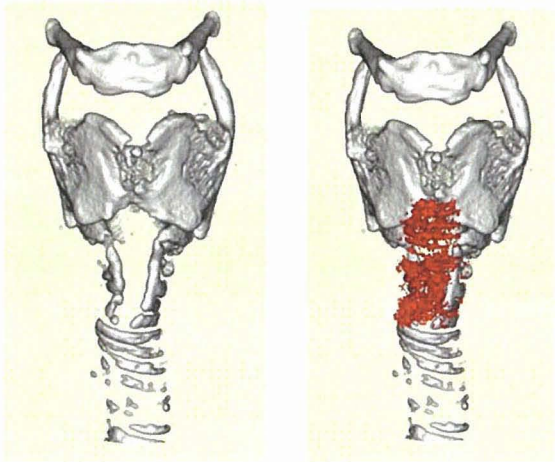

a　　b

図12．症例４：3DCT
ａ：術前
ｂ：術後（赤色部分は人工材料）

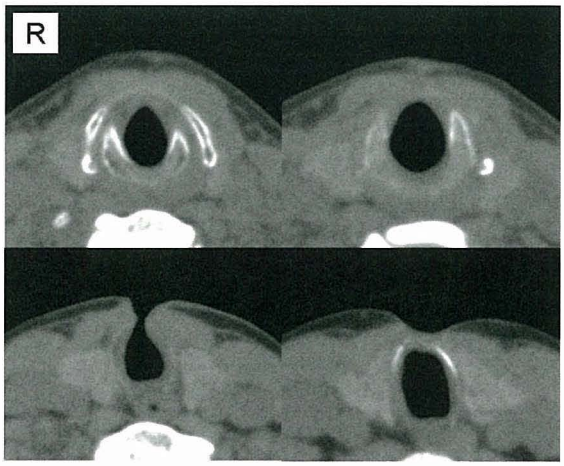

図13．症例５：術前 CT

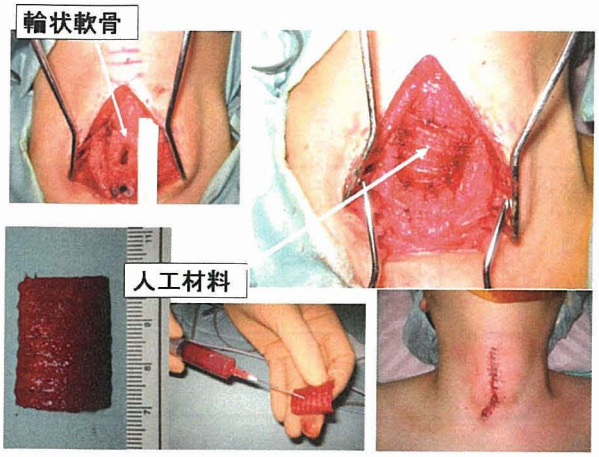

図14. 症例５：術中所見

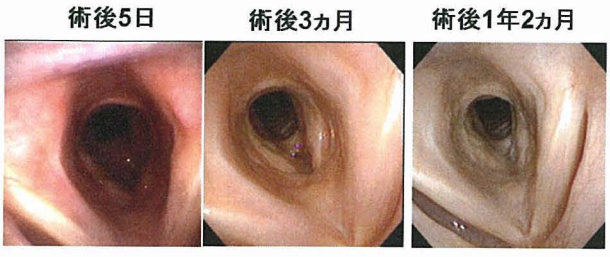

図15. 症例５：術後喉頭ファイバー所見
a：人工材料露出
b：上皮化あり
c：完全に上皮化

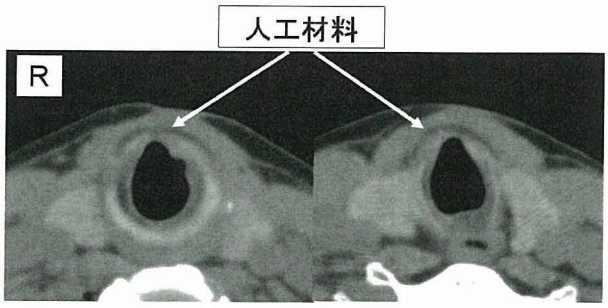

図16. 症例５：術後 CT
人工材料が lowdensity に描出
皮下気腫無し

表１．臨床応用例

症例	年齢	性別	診　断　名	術後観察期間	欠損の大きさ	気管内腔上皮化	術　後合併症	再狭窄
1	79	F	甲状腺癌再発	４年２ヶ月	気管軟骨１/２周・３リング	良好	無	無
2	71	M	甲状腺乳頭腺癌	３年１ヶ月	気管軟骨１/３周・２リング	良好	気腫	無
3	59	F	甲状腺癌再発	２年１ヶ月	輪状軟骨１／２周気管軟骨１/２周・２リング	良好	無	無
4	77	M	喉頭気管狭窄症	９ヶ月（他病死）	甲状軟骨の一部輪状軟骨１/３周気管軟骨１/２周・２リング	良好（一時肉芽あり）	無	無
5	42	F	特発性気管狭窄症	１年４ヶ月	気管軟骨１/３周・３リング	良好	無	無
6	29	F	外傷後の喉頭狭窄	１年２ヶ月	甲状軟骨の一部輪状軟骨１/３周	良好（一時肉芽あり）	無	無
7	29	F	特発性気管狭窄症	３ヶ月	甲状軟骨の一部輪状軟骨１/３周気管軟骨１/２周・３リング	良好（一時肉芽あり）	無	無

Ⅲ. 研究成果の刊行に関する一覧表

書　籍

著者氏名	論文タイトル名	書籍全体の編集者名	書籍名	出版社名	出版地	出版年	ページ
森野茂行, 永安　武, 中村達雄	細胞増殖因子と再生医療	松本邦夫, 田畑泰彦	肺気腫	メディカルレビュー社	大阪	2006	101～105

雑　誌

発表者氏名	論文タイトル名	発表誌名	巻号	ページ	出版年
Nagase H, Gren J, Saito A, Liu K, Agre P, Hazama A, Yasui M	Molecular cloning and characterization of mouse aquaporin 6	Biochem Biophys Res Commun	352	12～16	2007
Yamashita M, Omori K, Kanemaru S, Magrufov A, Tamura Y, Umeda H, Kishimoto M, Nakamura T, Ito J	Experimental regeneration of canine larynx: a trial with tissue engineering techniques	Acta Otolaryngol	557 Suppl	66～72	2007
Yamashita M, Kanemaru S, Hirano S, Magrufov A, Tamaki H, Tamura Y, Kishimoto M, Omori k, Nakamura T, Ito J	Tracheal regeneration after partial resection: A tissue engineering approach	Laryngoscope	117(3)	497～502	2007
Nakashima S, Nakamura T, Miyagawa K, Yoshikawa T, Kin S, Kuriu Y, Nakase Y, Sakakura C, Otsuji E, Hagiwara A, Yamagishi H	In situ tissue engineering of the bile duct using polypropylene mesh- collagen tubes	Int J Artif Organs in press			2007
Nakase Y, Nakamura T, Kin S, Nakashima S, Yoshikawa T, Kuriu Y, Miyagawa K, Sakakura C, Otsuji E, Ikada Y, Yamagishi H, Hagiwara A	Endocrine cell and nerve regeneration in autologous in situ tissue-engineered small intestine	J Surg Res	137	61～68	2007
Kobayashi K, Nomoto Y, Suzuki T, Tada Y, Miyake M, Hazama A, Kanemaru S, Nakamura T, Omori K	Effect of fibroblasts on tracheal epithelial regeneration in vitro	Tissue Eng	12(9)	2619～2628	2006
Nomoto Y, Suzuki T, Tada Y, Kobayashi K, Miyake M, Hazama A, Wada I, Kanemaru S, Nakamura T, Omori K	Tissue engineering for regeneration of the tracheal epithelium	Ann Otol Rhinol Laryngol	115(7)	501～506	2006
Katsuda S, Miyashita H, Takazawa K, Machida N, Kusanagi M, Miyake M, Hazama A	Mild hypertension in young Kurosawa and Kusanagi-hypercholesterolaemic (KHC) rabbits	Physiol Meas	27	1361～1371	2006
Matsuno T, Nakamura T, Kuremoto K, Notazawa S, Nakahara T, Hashimoto Y, Satoh T, Shimizu Y	Development of β-tricalcium phosphate/collagen sponge composite for bone regeneration	Dental Materials Journal	25	138～144	2006

発表者氏名	論文タイトル名	発表誌名	巻号	ページ	出版年
Morino S, Toba T, Araki M, Azuma T, Tsutsumi S, Tao H, Nakamura T, Nagayasu T, Tagawa T	Noninvasive assessment of pulmonary emphysema using dynamic contrast-enhanced magnetic resonance imaging	Exp Lung Res	32	55～67	2006
Nakase Y, Hagiwara A, Nakamura T, Kin S, Nakashima S, Yoshikawa T, Fukuda K, Kuriu Y, Miyagawa K, Sakakura C, Otsuji E, Shimizu Y, Ikada Y, Yamagishi H	Tissue engineering of small intestinal tissue using collagen sponge scaffolds seeded with smooth muscle cells	Tissue Eng	12	403～412	2006
Tao H, Araki M, Sato T, Morino S, Kawanami R, Yoshitani M, Nakamura T	Bronchoscopic treatment of postpneumonectomy bronchopleural fistula with a collagen screw plug	J Thorac Cardiovasc Surg	132	99～104	2006
Tanaka S, Takigawa T, Ichihara S, Nakamura T,	Mechanical properties of the bioabsorbable polyglycolic acid-collagen nerve guide tube	Polym Eng Sci	46	1461～1467	2006
大森孝一	喉頭疾患の治療：最近の話題	大阪府耳鼻咽喉科医会会報	66	23～44	2007
大森孝一，中村達雄，多田靖宏，野本幸男，鈴木輝久，小林　謙，佐藤　聡，金丸眞一，安里　亮，山下　勝	気道の再生と臨床応用	分子呼吸器病	10(3)	216～219	2006
大森孝一，中村達雄，多田靖宏，野本幸男，鈴木輝久，金丸眞一，安里　亮，山下　勝	甲状腺癌治療における気道の再生医療	再生医療	5(4)	545～549	2006
中村達雄	末梢神経の再生	治療	88	3028～3032	2006
稲田有史，中村達雄，諸井慶七郎，森本　茂	神経因性疼痛ならびにCRPS (Complex regional pain syndrome) に対する生体内再生治療	末梢神経	17	325～327	2006
萩原明於，阪倉長平，大辻英吾，山岸久一，中村達雄，清水慶彦	癌治療における神経再生の応用	再生医療	5	99～103	2006
大森孝一，多田靖宏，松塚　崇，野本幸男，鈴木輝久，中村達雄，金丸眞一，安里　亮，山下　勝，田中信三	喉頭・気管狭窄の再生治療	日本気管食道科学会会報	57(2)	153～154	2006

報道

医療材移植，気道を再生	日本経済新聞	2007年（平成19年）3月26日（月）日刊

Ⅳ. 研究成果の刊行物・別刷

Available online at www.sciencedirect.com
ScienceDirect
Biochemical and Biophysical Research Communications 352 (2007) 12–16
BBRC
www.elsevier.com/locate/ybbrc

Molecular cloning and characterization of mouse aquaporin 6

Hiroaki Nagase [a,1], Johan Ågren [a,2], Akiko Saito [b], Kun Liu [a,3], Peter Agre [a,4], Akihiro Hazama [b], Masato Yasui [a,*]

[a] *Department of Biological Chemistry, Johns Hopkins University School of Medicine, 725 N. Wolfe St. Baltimore, MD 21205-2185, USA*
[b] *Department of Physiology, Fukushima Medical University School of Medicine, 1 Hikarigaoka, Fukushima City, 960-1247, Japan*

Received 15 October 2006
Available online 30 October 2006

Abstract

In the rat kidney, aquaporin (AQP) 6 is localized in the intracellular vesicle membranes of type-A intercalated cells of the collecting duct; mouse AQP6 (mAQP6) has not been characterized. Although mAQP6 was originally cloned from cDNA in a mouse cerebellum library (GenBank NM 175087), we have independently cloned a cDNA encoding mAQP6 from an adult kidney cDNA library (C57BL/6J strain). We identified two different spliced variants of mAQP6: mAQP6a and mAQP6b. The mAQP6a isoform is almost identical to that of rat AQP6, whereas mAQP6b is identical to that reported in the mouse cerebellum library mentioned above. We found that the mRNA expression of these two spliced variants is regulated in a tissue-specific and age-dependent manner. Functional analyses of water and ion permeation revealed that mAQP6a functions like rat AQP6 and that mAQP6b does not function as either a water channel or an ion channel under our experimental conditions.

Keywords: Aquaporin; Splice variant

The aquaporins (AQPs) are a family of membrane proteins that largely function as water channels [1]. In mammals, 13 members of the AQP family (AQP0-12) have been reported [2]. AQP6 has been isolated from rat and human kidneys [3,4], and in rat studies we have shown that AQP6 is functionally distinct from other known AQPs in the following ways. First, AQP6 is localized in intracellular membranes in type-A intercalated cells of the kidney [5]. Second, AQP6 functions not as a water channel but as an anion channel [5–7]: ion permeability, including that of hydronium ions, is not a general feature of AQPs [7,8]. Third, AQP6 is activated by Hg^{2+}, a well-known water channel inhibitor [1]. AQP6 has also been cloned from mouse cDNA (GenBank NM 175087) derived from the cerebellum. Interestingly, we found that the C-terminal domain of this clone exhibits no significant homology to known sequences of rat or human AQP6; also, no rat or human AQP6 has been reported in the cerebellum. Furthermore, no studies to date have examined the function of mouse AQP6 (mAQP6). To address these issues and provide a foundation for further studies of AQP6, we independently cloned mAQP6 from an adult kidney cDNA library (C57BL/6J strain). We identified two spliced variants of mAQP6. The two isoforms display distinct tissue-specific distribution, developmental regulation, and functional characteristics.

Materials and methods

Isolation of mAQP6 isoforms. Primers for the full-length of the mAQP6 coding region were designed from the cDNA retrieved from GenBank

* Corresponding author. Present address: Department of Pharmacology, Keio University School of Medicine, 35 Shinanomachi, Shinjuku, Tokyo 160-8582, Japan. Fax: +81 3 3359 8889.
E-mail address: myasui@sc.itc.keio.ac.jp (M. Yasui).
[1] Present address: Deaprtment of Pediatric Neurology, Kobe Children's Hospital, Kobe, Hyogo, Japan.
[2] Present address: Department of Women's and Children's Health, Uppsala University, Uppsala, Sweden.
[3] Present address: Trimgen Genetic Diagnostics, Sparks, MD, USA.
[4] Present address: Department of Cell Biology, Duke University School of Medicine, Durham, NC, USA.

0006-291X/$ - see front matter © 2006 Elsevier Inc. All rights reserved.
doi:10.1016/j.bbrc.2006.10.110

(Accession No. NM 175087) with the *Eco*RI site as the upstream primer and the *Nhe*I site as the downstream primer. The sequence of the upstream primer was 5′-ATAGAATTCCATGGAGCCAGGGCTGTGTAGC-3′ and that of the downstream primer was 5′-AATAGCTAGCTCAG CAAAGGCCAAGCGTGAATG-3′. All animal experiments were conducted under protocols approved by the Johns Hopkins Animal Care and Use Committee. Total RNA was extracted from the kidneys of adult (3–4-month-old) C57BL/6J mice using the RNeasy kit with optional DNase treatment (Qiagen, Valencia, CA). An aliquot of 5 μg of total RNA was then used for cDNA synthesis with the SuperScript First-Strand Synthesis System for RT-PCR (Invitrogen, Carlsbad, CA), and 2.5 μL of the resulting cDNAs was subsequently amplified using the Expand High Fidelity PCR system (Roche Applied Science, Penzberg, Germany). All PCR products were purified with a Qiaquick Gel Extraction Kit (Qiagen) and subcloned into the multiple cloning regions of pXβG-myc and pcXβG3 vectors at the *Eco*RI and *Nhe*I sites. The pcXβG3 vector had been constructed by cloning the *Xenopus* β-globin 5′- and 3′- untranslated regions into the pcDNA3 vector (and was kindly supplied by Michael Caterina, Johns Hopkins University, Baltimore, MD, USA). The pXβG-myc vector was constructed by adding a c-myc tag at the *Bgl*I site of the pXβG vector. Sequencing was used to verify the DNA sequence of the constructs.

Analysis of mAQP6 mRNA expression using RT-PCR. RNA extraction and RT-PCR were performed as described above using cerebella and kidneys from 1-day-old (P1) and adult mice. This time 2 μL of the resulting cDNAs was amplified with primers synthesized according to the sequence of mAQP6 cDNA. The upstream primer used for mAQP6 cDNA was 5′-ACTGGCTGTTCCATGAACCC-3′, and the downstream primer was 5′-AGGAAGTGGCCAGGAGGTACT-3′. The PCR were cycled 40 times, using a 1-min, 94 °C denaturing step; a 1-min, 61 °C annealing step; and a 1-min, 72 °C extension step. The PCR products were visualized by ethidium bromide staining and electrophoresis in 2% agarose.

Expression in oocytes and measurement of P_f. Capped cRNAs were synthesized in vitro from *Xba*I-linearized pcXβG3 plasmids with T7 RNA polymerase and purified with the RNeasy kit (Qiagen). Five nanograms (50 nL) of cRNA or 50 nL of diethyl pyrocarbonate-treated water was injected into defolliculated mature *Xenopus laevis* oocytes (controls). The oocytes were incubated for 2–3 days at 18 °C in 200 mOsm modified Barth's solution (MBS). An oocyte-swelling assay was used to measure osmotic water permeability (P_f) was measured from the time course of oocytes swelling in response to a 3-fold dilution of MBS with distilled water as in previous studies [9]. For Hg^{2+} studies, oocytes were preincubated for 5 min in 200 mOsm MBS containing 0.5 mM $HgCl_2$ before the swelling assay, whereas the controls were preincubated without $HgCl_2$.

Oocyte immunofluorescence and confocal microscopy. Three days after injection oocytes were incubated in fixing solution (80 mM Pipes, pH 6.8, 5 mM EGTA, 1 mM $MgCl_2$, 3.7% formaldehyde, and 0.2% Triton X-100) at room temperature for 4 h, transferred to methanol at −20 °C for 24 h, equilibrated in PBS at room temperature for 2 h, incubated in PBS with 100 mM $NaBH_4$ at room temperature for 24 h, and bisected with blades. The oocytes were blocked by 2% BSA in PBS for 1 h at room temperature, incubated at 4 °C sequentially with rabbit anti-AQP6 antibody [10] and Alexa Fluor 488 goat anti-rabbit IgG (Invitrogen) in blocking buffer (each for 24 h), and mounted in Fluoromount-G (SouthernBiotech, Birmingham, AL, USA). Micrographs were obtained with a confocal laser-scanning microscope (UltraView LCI, Perkin-Elmer, Wellesley, MA, USA).

Oocyte membrane extraction and immunoblotting. Ten oocytes were homogenized by pipetting them up and down in hypotonic lysis buffer (7.5 mM sodium phosphate, 1 mM EDTA, pH 7.5) including a protease inhibitor mixture (Sigma–Aldrich, St. Louis, MO, USA). The oocyte yolk was removed by discarding the pellet after centrifugation at 735*g* and 4 °C for 10 min. The supernatant was centrifuged again at 200,000*g* and 4 °C for 1 h; the membrane was harvested by collecting the pellet. The oocyte membrane was solubilized with 2% SDS, normalized by total protein amount following the BCA method (Pierce, Rockford, IL, USA), and subjected to 12% SDS–PAGE. The proteins were transferred to a poly-vinylidene-difluoride) membrane, probed with a rabbit anti-rat AQP6 antibody and a horseradish peroxidase-conjugated donkey anti-rabbit IgG (Amersham Biosciences, Pittsburgh, PA, USA). An enhanced chemiluminescence detection system (ECL-plus, Amersham Biosciences) was used to visualize the specific immunoreactive proteins by exposure to autoradiographic films.

Electrophysiological measurements of oocytes were performed with iso-osmotic. NaCl solution (100 mM NaCl, 2 mM KCl, 1 mM $MgCl_2$, and 5 mM Hepes, pH 7.5) or iso-osmotic $NaNO_3$ solution (100 mM $NaNO_3$, 2 mM KCl, 1 mM $MgCl_2$, and 5 mM Hepes, pH 7.5). The membrane potential of oocytes was controlled by the two-microelectrode voltage clamp technique. The command voltage was applied with a two-microelectrode voltage clamp amplifier (Axoclamp-2A, Axon Instruments, Foster City, CA) controlled by an IBM-compatible computer running pCLAMP software (Axon Instruments). Current signals were sampled at 100 μs. In most experiments the membrane potential was held at $V_{hold} = -50$ mV. To determine the current–voltage relationship, the membrane potential was rapidly stepped up from the holding potential to a series of values generating between +50 and −130 mV, each differing by 20 mV. The pulse duration was 100 ms, and currents from 10 runs were averaged to reduce noise. All measurements were performed at room temperature.

Results

By RT-PCR experiments using mouse kidney cDNA as a template, we obtained two different full-length cDNA fragments. One of them (named mAQP6a) (GenBank DQ 826418) was almost identical to rAQP6, whereas the other clone (named mAQP6b) was identical to the previously reported mAQP6 (GenBank NM 175087). The mAQP6a cDNA results from a retention of intron 4, creating a novel 3′ end (Fig. 1A). Nucleotide sequencing analysis revealed that the mAQP6 gene encodes proteins with 276 and 293 amino acid residues and that the difference is observed only at the C-terminus (Fig. 1B). The mAQP6b C-terminal domain exhibits no significant homology to known sequences from other AQPs.

Expression of mAQP6 in the cerebellum and kidney

To investigate the age-related and tissue-specific expression of mAQP6a and mAQP6b, we performed RT-PCR with primers that are designed to amplify 727-bp and 364-bp fragments for mAQP6a and mAQP6b, respectively (Fig. 2). In the cerebellum, mAQP6b was detected only in P1 mice, from which mAQP6b was originally cloned, whereas mAQP6a was expressed not in the P1 but in the adult cerebellum. In the kidney, mAQP6a, and mAQP6b were expressed in both P1 and adult mice. Expression of mAQP6a was higher in adult mice, in both the cerebellum and kidney.

Functional studies

The functional properties of mAQP6 were evaluated by expression in *Xenopus* oocytes. Swelling was monitored after the oocytes had been transferred from 200 to 70 mOsm modified Barth's solution, and the coefficients of osmotic water permeability (P_f) were calculated. Like

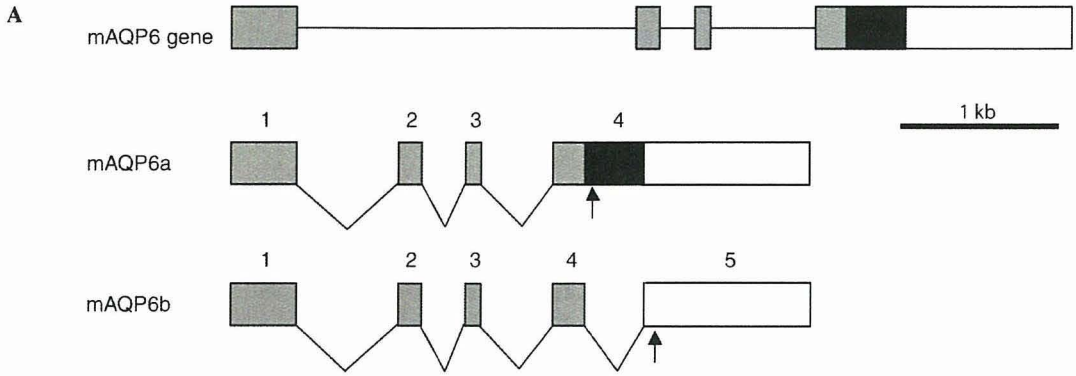

B

rAQP6	1	MEPGLCNRAYLLVGGLWTAISKALFAEFLATGLYVFFGVGSVLPWPVALP	50	rAQP6
mAQP6a	1	MEPGLCSRAYLLVGGLWTAISKALFAEFLATGLYVFFGVGSVLPWPVALP	50	mAQP6a
mAQP6b	1	MEPGLCSRAYLLVGGLWTAISKALFAEFLATGLYVFFGVGSVLPWPVALP	50	mAQP6b
rAQP6	51	SVLQVAITFNLATATAVQISWKTSGAHANPAVTLAYLVGSHISLPRAVAY	100	rAQP6
mAQP6a	51	SVLQIAITFNLATATAVQISWKTSGAHANPAVTLAYLVGSHISLPRAMAY	100	mAQP6a
mAQP6b	51	SVLQIAITFNLATATAVQISWKTSGAHANPAVTLAYLVGSHISLPRAMAY	100	mAQP6b
rAQP6	101	IAAQLAGATVGAALLYGVTPGGVRETLGVNVVHNSTSTGQAVAVELVLTL	150	rAQP6
mAQP6a	101	IAAQLAGATAGAALLYGVTPGGIRETLGVNVVHNSTSTGQAVAVELVLTL	150	mAQP6a
mAQP6b	101	IAAQLAGATAGAALLYGVTPGGIRETLGVNVVHNSTSTGQAVAVELVLTL	150	mAQP6b
rAQP6	151	QLVLCVFASMDSRQTLGSPAAMIGTSVALGHLIGIYFTGCSMNPARSFGP	200	rAQP6
mAQP6a	151	QLVLCVFASMDGRQTLASPAAMIGTSVALGHLIGIYFTGCSMNPARSFGP	200	mAQP6a
mAQP6b	151	QLVLCVFASMDGRQTLASPAAMIGTSVALGHLIGIYFTGCSMNPARSFGP	200	mAQP6b
rAQP6	201	AVIVGKFAVHWIFWVGPLTGAVLASLIYNFILFPDTKTVAQRLAILVGTT	250	rAQP6
mAQP6a	201	AVIVGKFAVHWIFWVGPLTGAVLASLIYNFILFPDTKTVAQRLAILVGTT	250	mAQP6a
mAQP6b	201	AVIVGKFAVHWIFWVGPLTGAVLASLIYNFILFPDTKTVAQRLAILVGTT	250	mAQP6b
rAQP6	251	KVEKVVDLEPQKKESQTNSEDTEVSV	276	rAQP6
mAQP6a	251	KVEKVVDLEPQKKESQTNSEDTEVSV	276	mAQP6a
mAQP6b	251	KVEKVVDLEPQKKESQTNSEDTECLTSPCEEAVRSFSFTLGLC	293	mAQP6b

Fig. 1. Isolation of mAQP6 splicing variants. (A) Exon–intron organization of the mouse AQP6 gene. A segment of the genomic *AQP6* clone is shown at the top of the figure. The gray rectangles represent common translated regions of AQP6. Exon 4 of mAQP6a contains a black rectangle with a stop codon in it (arrow). mAQP6b has another intron (intron 4) and exon 5; the stop codon is in exon 5. (B) Sequence alignments of rat AQP6, mAQP6a, and mAQP6b. The blue residues are identical. Red NPAs are a motif of AQPs. (For interpretation of the references to colour in this figure legend, the reader is referred to the web version of this article.)

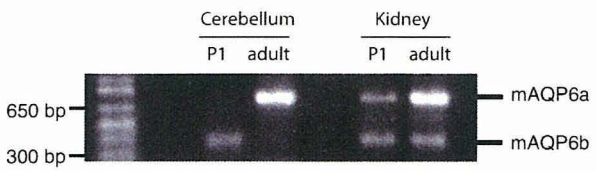

Fig. 2. Developmental regulation of mAQP6 transcripts. RT-PCR analysis of mAQP6 expression in the mouse kidney and cerebellum. Total RNA of different developmental points; neonatal (P1) and adult mice subjected to RT-PCR using specific primers for mAQP6.

rAQP6, mAQP6a has low water permeability, which is activated by Hg^{2+} (Fig. 3A). On the other hand, Hg^{2+} does not activate mAQP6b, which also has low basal water permeability. We evaluated the ionic permeation of oocytes expressing mAQP6 using a two-electrode voltage clamp. Oocytes expressing mAQP6a exhibit current under Hg^{2+} treatment, which is also the case with of oocytes expressing rAQP6 (Fig. 3B). On the other hand, of oocytes expressing mAQP6b did not exhibit any current either with or without Hg^{2+} treatment. Confocal microscopy demonstrated that both mAQP6a and mAQP6b are located at the oocyte plasma membrane (Fig. 4A). It should be noted that the anti-AQP6 antibody recognized a 30-kDa and a 28-kDa band from oocytes into which mAQP6a had been injected and also recognized a 31-kDa and a 29-kDa band from oocytes into which mAQP6b had been injected (Fig. 4B).

Discussion

We have previously characterized rat AQP6 [5–7,10] and found that it is localized in the acid-secreting cells of the renal collecting ducts [10] and functions as an anion channel [5–7]. Mouse AQP6 was cloned from a cerebellum library during a large-scale full-length cDNA expression analysis in mice carried out by RIKEN as part of the FANTOM project (GenBank NM 175087) [11,12]. The FANTOM project represents one of the most comprehensive surveys of a mammalian transcriptome using a full-length cDNA set. However, as was pointed out at the time, it is necessary to perform experimental analyses to verify

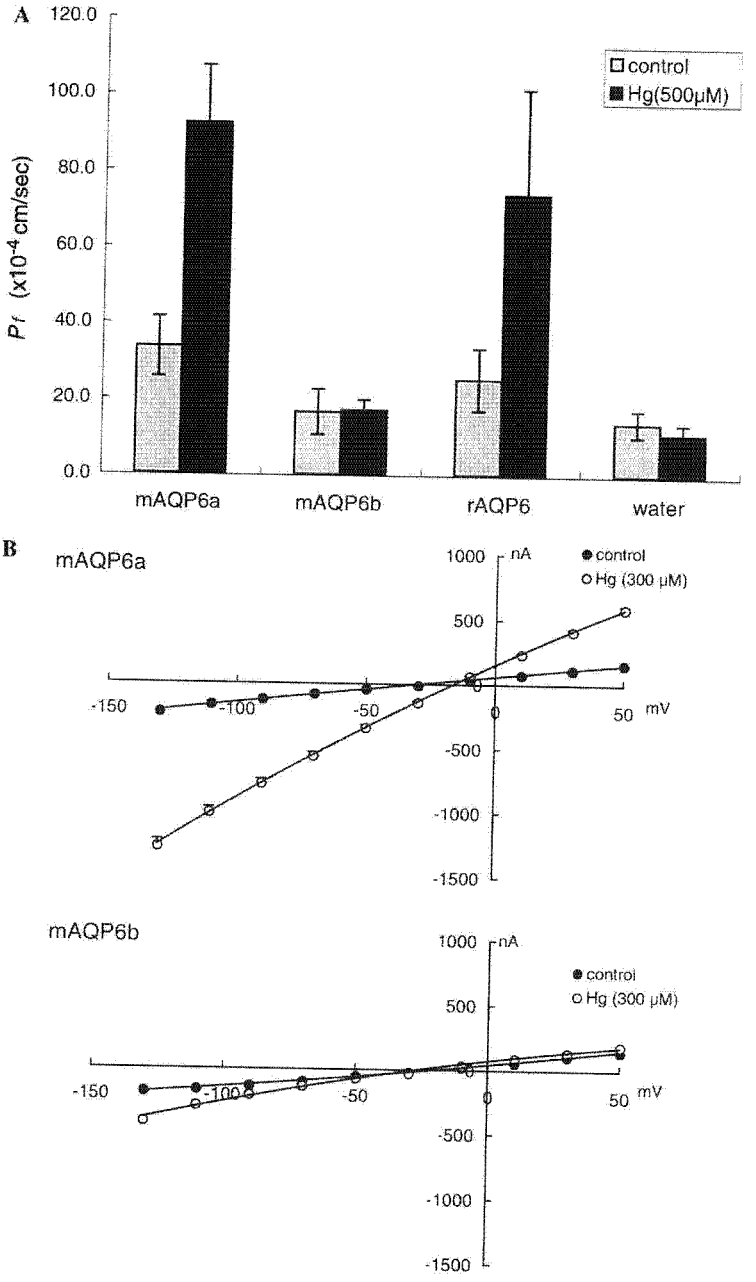

Fig. 3. (A) The coefficient of osmotic water permeability (P_f) of mAQP6a, mAQP6b, and rAQP6. Mercury treatment activated water permeability in mAQP6a and rAQP6 but not in mAQP6b. (B) Electrophysiological analyses of mAQP6a and mAQP6b. One-volt curves between +50 and −130 mV were plotted for data obtained from mAQP6a (upper panel) and mAQP6b (lower panel) oocytes. Electrophysiological experiments were performed with a two-electrode voltage clamp system. The membrane potential was held at −50 mV and rapidly stepped up to test potentials from +50 to −130 mV at 20-mV intervals. Currents at each voltage were measured with pClamp software.

the functions of genes predicted by computational analyses. The primary sequence revealed that this clone is very different from that of rat or human AQP6. In this study we independently cloned and characterized mAQP6. We found that a new spliced variant of mAQP6 resulted from intron retention and an alternative in-frame stop codon. The new isoform (termed mAQP6a) is almost identical to rat AQP6, whereas the other clone (here called mAQP6b), which has a different C-terminal amino acid, is identical to the one reported in the RIKEN study. Interestingly, we found that both function and distribution differ between mAQP6a and mAQP6b. Sequence homology showed that when expressed in oocytes mAQP6a, like rat AQP6, is activated by Hg^{2+} and permeated by ions, whereas mAQP6b does not function either as a water channel or an ion channel. The abundance of mAQP6b in neonatal mouse

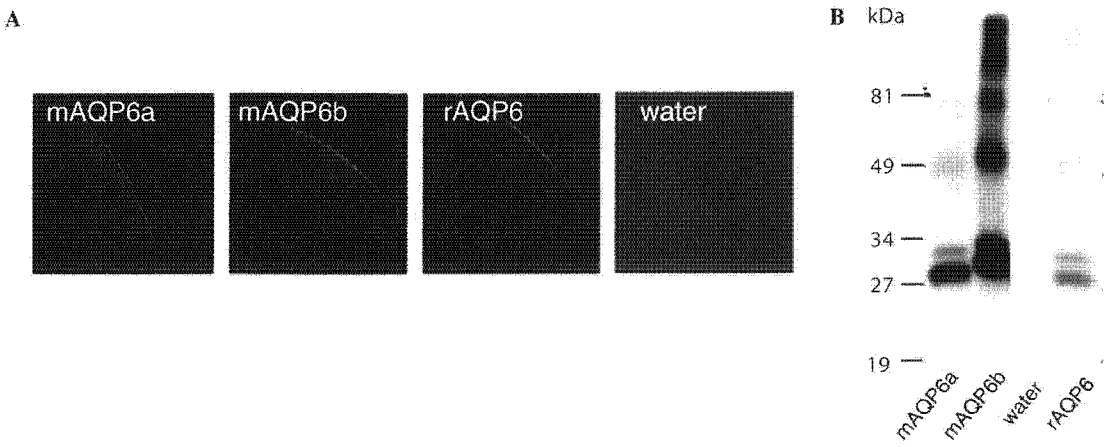

Fig. 4. mAQP6/rAQP6 expressed in oocytes. (A) Confocal microscope images of oocytes into which water, mAQP6a, mAQP6b, or rAQP6 had been injected. The oocytes were stained with an anti-rat AQP6 antibody. (B) Immunoblotting of membrane fractions from oocytes into which mAQP6a, mAQP6b, water, or rAQP6 had been injected.

cerebella is consistent with the isolation of the previously reported mouse AQP6 clone from the cerebella of neonatal mice.

We also found that the expression of the mRNA of these two splicing variants is regulated in a tissue-specific and age-related manner, suggesting that mAQP6 may be important during development. The expression of mAQP6a and mAQP6b in the cerebellum is provocative. Immunocytochemical studies with mAQP6-specific antibodies will be needed to determine the physiological relevance of AQP6 to cerebellar function.

Functional analysis revealed that mAQP6a functions as an anion channel, as does rat AQP6. Although mAQP6b was expressed in the plasma membranes of oocytes, we could not demonstrate any water or ion transport. Thus, the biological function of mAQP6b remains unclear. The C-terminus of mAQP6b has a putative casein kinase II phosphorylation site at Ser 277, which may regulate channel gating. One could speculate that mAQP6b forms a heterologous oligomer with mAQP6a, which may have a dominant negative effect on both proteins. However, when mAQP6a and mAQP6b were expressed together in oocytes, no dominant negative effects were detected (data not shown).

Our immunofluorescence studies revealed that both mAQP6a and mAQP6b are expressed in the plasma membranes of oocytes. Although the C-terminus of rat AQP6 is presumably less important for trafficking than is the N-terminus [6], these two isoforms might traffic differently when expressed in mammalian cells. To clarify the precise distribution of mAQP6b, we plan to develop an antibody that recognizes mAQP6b but not mAQP6a. mAQP6b may have distinct cellular distributions and functions during development.

Acknowledgments

This work was supported by a Grant DK065098 from National Institution of Health, and Ministry of Education, Science, Sports and Culture. Grant-in Aid for Scientific Research (C) 15590902, Japan.

References

[1] P. Agre, L.S. King, M. Yasui, W.B. Guggino, O.P. Ottersen, Y. Fujiyoshi, A. Engel, S. Nielsen, Aquaporin water channels—from atomic structure to clinical medicine, J. Physiol. 542 (2002) 3–16.
[2] T. Itoh, T. Rai, M. Kuwahara, S.B. Ko, S. Uchida, S. Sasaki, K. Ishibashi, Identification of a novel aquaporin, AQP12, expressed in pancreatic acinar cells, Biochem. Biophys. Res. Commun. 330 (2005) 832–838.
[3] T. Ma, A. Frigeri, W. Skach, A.S. Verkman, Cloning of a novel rat kidney cDNA homologous to CHIP28 and WCH-CD water channels, Biochem. Biophys. Res. Commun. 197 (1993) 654–659.
[4] T. Ma, B. Yang, W.L. Kuo, A.S. Verkman, cDNA cloning and gene structure of a novel water channel expressed exclusively in human kidney: evidence for a gene cluster of aquaporins at chromosome locus 12q13, Genomics 35 (1996) 543–550.
[5] M. Yasui, A. Hazama, T.H. Kwon, S. Nielsen, W.B. Guggino, P. Agre, Rapid gating and anion permeability of an intracellular aquaporin, Nature 402 (1999) 184–187.
[6] M. Ikeda, E. Beitz, D. Kozono, W.B. Guggino, P. Agre, M. Yasui, Characterization of aquaporin-6 as a nitrate channel in mammalian cells. Requirement of pore-lining residue threonine 63, J. Biol. Chem. 277 (2002) 39873–39879.
[7] A. Hazama, D. Kozono, W.B. Guggino, P. Agre, M. Yasui, Ion permeation of AQP6 water channel protein. Single channel recordings after Hg^{2+} activation, J. Biol. Chem. 277 (2002) 29224–29230.
[8] N. Chakrabarti, B. Roux, R. Pomes, Structural determinants of proton blockage in aquaporins, J. Mol. Biol. 343 (2004) 493–510.
[9] G.M. Preston, T.P. Carroll, W.B. Guggino, P. Agre, Appearance of water channels in *Xenopus* oocytes expressing red cell CHIP28 protein, Science 256 (1992) 385–387.
[10] M. Yasui, T.H. Kwon, M.A. Knepper, S. Nielsen, P. Agre, Aquaporin-6: an intracellular vesicle water channel protein in renal epithelia, Proc. Natl. Acad. Sci. USA 96 (1999) 5808–5813.
[11] J. Kawai et al., Functional annotation of a full-length mouse cDNA collection, Nature 409 (2001) 685–690.
[12] Y. Okazaki et al., Analysis of the mouse transcriptome based on functional annotation of 60,770 full-length cDNAs, Nature 420 (2002) 563–573.

Acta Oto-Laryngologica 2007; Suppl 557: 66–72

informa
healthcare

Experimental regeneration of canine larynx: a trial with tissue engineering techniques

MASARU YAMASHITA[1], KOICHI OMORI[2], SHIN-ICHI KANEMARU[1], AKHMAR MAGRUFOV[1], YOSHIHIRO TAMURA[1], HIROO UMEDA[1], MASANAO KISHIMOTO[1], TATSUO NAKAMURA[3], & JUICHI ITO[1]

[1]*Department of Otolaryngology-Head and Neck Surgery, Graduate School of Medicine, Kyoto University, Kyoto,* [2]*Department of Otolaryngology, Fukushima Medical University, Fukushima and* [3]*Department of Bioartificial Organs, Institute for Frontier Medical Sciences, Kyoto University, Kyoto, Japan*

Abstract

Conclusion: Since this tissue engineering technique is cost-effective and is less invasive to patients, it may replace conventional approaches in laryngeal reconstructive surgeries. *Objective:* Laryngeal cancer is one of the most prevalent cancers in the head and neck region, and frequently requires surgical resection. Although there are many ways to reconstruct the larynx after resection, donor tissue is usually required. Recently, tissue engineering techniques have become widely accepted in clinical medicine and have already been applied to some organs. This animal experiment was designed to elucidate the efficacy of laryngeal regeneration using tissue engineering technique. *Materials and methods:* A bioartificial scaffold was designed from a replica of a canine larynx. A dental cast was used to replicate the intricate inside shape of the larynx. After copying its shape on a polypropylene mesh sheet, this sheet was coated with spongy collagen from porcine skin. A hemilaryngectomy was performed on beagle dogs under general anesthesia. Then the scaffold, preclotted with a mixture of peripheral blood and bone marrow-derived stromal cells, was implanted and fixed. The postoperative status was examined fiberscopically. *Results:* On the eighth day after the operation, the surface of the implant was covered with soft tissue. Finally, the implant was completely covered with regenerated mucosa.

Keywords: *Laryngeal regeneration, tissue engineering, bioartificial scaffold, polypropylene, bone marrow-derived stromal cells*

Introduction

Although many approaches are available for laryngeal reconstruction after partial resection and physicochemical damage, such as the use of autologous tissue, allografts, and artificial materials, a reliable and standard model has yet to be established. For complete reconstruction of the larynx, anatomical configuration and functions have to be restored, rendering the task challenging.

Recently, remarkable progress has been achieved in regenerative medicine; highly differentiated tissues and certain organs can now be regenerated under appropriate conditions, using tissue engineering techniques [1–3]. These techniques routinely require three fundamental components: cells, scaffold (a cell-ingrowth transplant medium for regeneration), and growth regulation factors. Of these, the scaffold on which cells are grown is particularly important for regenerating tissues and organs.

In structure–function relationships, the larynx is not an exception in terms of its status as an organ. If an appropriate scaffold was prepared, regeneration of the larynx would be facilitated. In this study, laryngeal regeneration was attempted in dogs with a novel approach using a canine-replicated scaffold innovated with bone marrow-derived stromal cells (BSCs).

Materials and methods

Preparation of scaffolds and media for cell growth

A single sheet of polypropylene mesh with a pore size of 260 μm (Marlex mesh®; CR Bard, Billerica, MA,

Correspondence: Shin-ichi Kanemaru, MD, PhD, Department of Otolaryngology-Head and Neck Surgery, Graduate School of Medicine, Kyoto University, 54 Kawara-cho, Syogoin, Sakyo-ku, Kyoto 606-8507, Japan. Tel: +81 75 751 3346. Fax: +81 75 751 7225. E-mail: kanemaru@ent.kuhp.kyoto-u.ac.jp

ISSN 0365-5237 print/ISSN 1651-2551 online
DOI: 10.1080/00016480601068014

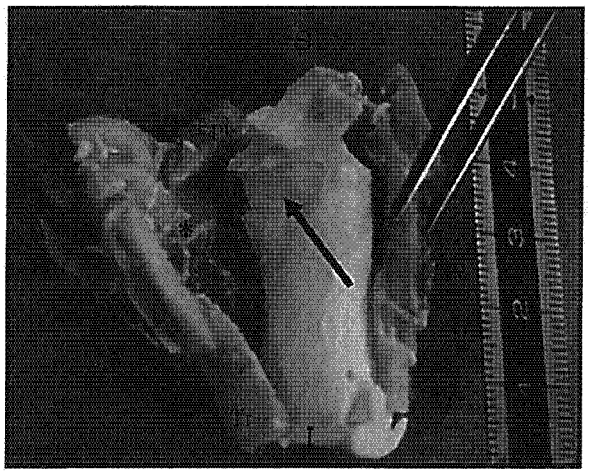

Figure 1. After the casting procedure, the cast lies on the right luminal surface of the larynx. A section was cut on the posterior side of the larynx with the left side of the larynx opened for viewing. The arrow shows an impressed shape of the left vocal fold (*) on a dental cast. Epi, epiglottis; Tr, trachea; S, superior; I, inferior; R, right; L, left.

USA) was used as the scaffold ground-framework. A female beagle dog (body weight 12 kg) employed as a control in a previous study was sacrificed, and the larynx was isolated. The shape of the larynx was then impressed with inpours from a dental cast (Neoprimestone®, Mutsumi Chemical Industries, Mie, Japan) (Figure 1). The anatomical contours were then molded accordingly on a polypropylene mesh sheet with heat (100°C, 1 h) using a drying sterilizer (SG-61, Yamato Scientific, Tokyo, Japan).

Another flat polypropylene mesh sheet (see above) was layered on the scaffold to structurally reinforce and firmly maintain its shape before fixation with fine polypropylene filaments (Figure 2A). A 1% porcine dermal atelocollagen (supplied by Nippon Meatpackers, Ibaraki, Japan) preparation comprising type I (70%) and type III (30%) collagens dissolved in aqueous hydrochloric acid (HCl, pH 3.0) was coated on both sides of the fixed polypropylene mesh sheets. After collagen-coating, freeze-drying with a freeze dryer (FDU-810, Tokyo Rikakikai, Tokyo, Japan), and cross-linkage with a vacuum dry oven (VOS-300SD, Tokyo Rikakikai) were applied to the scaffold to facilitate cellular attachment and ingrowth (Figure 2B).

Preparation of BSCs

Bone marrow extract (approx. 2 ml) obtained from the left humerus of each animal with an extractor, was placed in an 80 cm^2 culture bottle and incubated with Dulbecco's modified Eagle medium containing 10% fetal bovine serum and antibiotics (penicillin G Na 10000 units/ml, streptomycin sulfate 10000 μg/ml, and 25 μg/ml amphotericin B as fungizone in 0.85% saline; Invitrogen, Carlsbad, CA, USA) at 37°C under 5% CO_2 atmosphere.

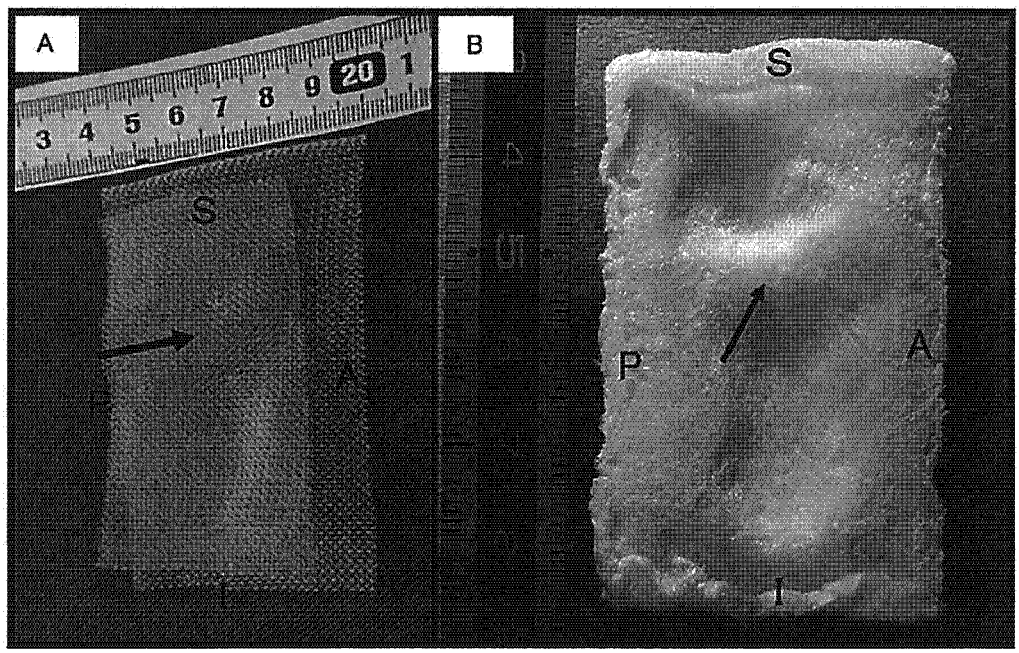

Figure 2. (A) The affected contours of a vocal fold on a polypropylene mesh are indicated by an arrow. The inner side mesh was reinforced by an overlying flat mesh sheet. (B) A luminal view of the scaffold after collagen treatment with the level of the resected vocal fold indicated by an arrow. S, superior; I, inferior; A, anterior; P, posterior.

After removal of the floating cells by aspiration, those attached on the bottom of the bottle were incubated in the fresh medium described above for 1 month without passage. Replacements of medium were regularly repeated with fresh portions at 3-day intervals. Attached cells were collected by trypsin treatment ($1.0–2.0 \times 10^6$ cells) and used as BSCs.

Animals and surgical procedures

Animal care, housing, and experimental procedures were conducted according to the Guideline for Animal Experiments of Kyoto University. Three adult beagle dogs (X, Y, and Z), each weighing 12–14 kg, were anesthetized with ketamine HCl (5.0 mg/kg; Sankyo, Tokyo, Japan) and xylazine HCl (2.0 mg/kg; Bayer, Tokyo, Japan) followed by tracheal intubation. The animals were then generally anesthetized with a mixture of oxygen, nitrous oxide, and halothane before left vertical hemilaryngectomy (Figure 3), approx. 2.5 cm × 2 cm in size, using a scalpel. A scaffold implant, preclotted with 5 ml of arterial blood containing BSCs, was trimmed according to the defect size during the operation (Figure 4). The clotting procedure rendered the implant completely infiltrated with BSCs and neutralized any air spaces from causing leakage and/or hindering cell growth. The fully prepared scaffold for each experimental animal was anastomosed according to resected boundaries of the defect and arytenoid cartilage with 3–0 absorbable sutures (Vicryl®; Ethicon, Somerville, NJ, USA) (Figure 5). Ampicillin sodium (Meiji Seika Kaisha, Tokyo, Japan) was administered (250 mg/animal; s.c.) for 3 days, followed by daily oral 500 mg doses for 2 weeks to prevent postoperative infections.

Outcome assessment

Endoscopic examinations to monitor progress of regenerative status were undertaken periodically. Anesthesia was induced with ketamine HCl and xylazine HCl (see above) to facilitate these examinations. The luminal status was examined with a video-endoscopy system consisting of a video bronchoscope (BF type 1T240, Olympus, Tokyo, Japan) and a video processor (CV-240, Olympus) with a light source (CLV-U40D, Olympus).

Images were portrayed via computed tomography (CT) performed on the operated site using a helical CT scanner system (Legato Duo, GE Yokogawa Medical Systems, Tokyo, Japan).

Results

The postoperative conditions of two dogs (X and Z) were normal, while the remaining dog (Y) died of unknown causes 4.5 months after the operation.

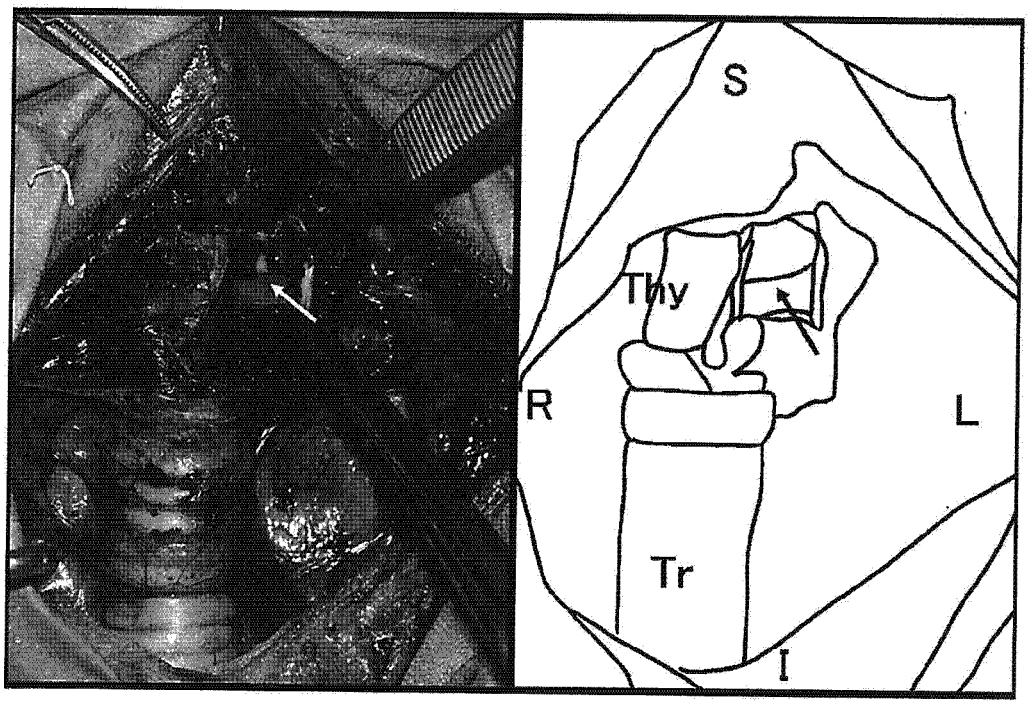

Figure 3. A left vertical hemilaryngectomy (left panel) performed on the larynx was simplified with an illustrative diagram (right panel) for reference. The arrows indicate the left vocal folds. Thy, right ala of the thyroid cartilage; Tr, trachea; S, superior; I, inferior; R, right, L, left.

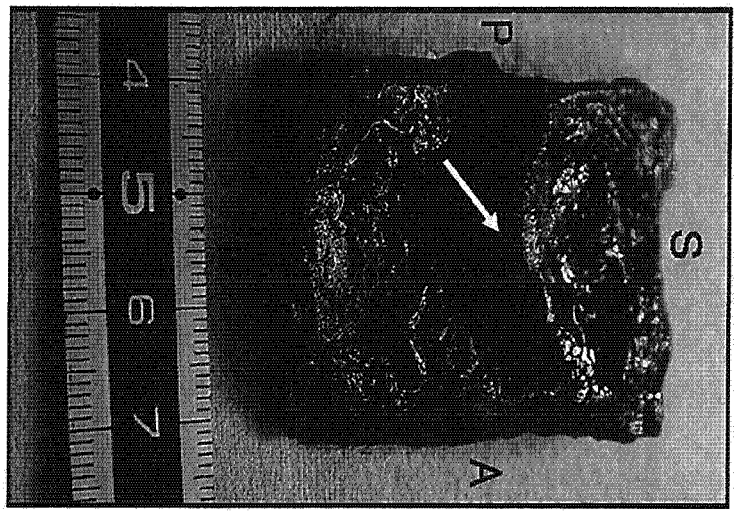

Figure 4. The level of the vocal cord after the preclotting procedure. S, superior; I, inferior; A, anterior; P, posterior.

Dog X was sacrificed 1 year after the operation. The local fiberscopic findings of the three dogs are summarized in Table I.

Fiberscopic images of operative events in dog Z (Figures 6 and 7) with typical luminal portrayals of a successfully reconstructed larynx at 20 months post-operatively (Figure 7) compared with the preoperative image of a normal larynx (Figure 6A). The preclotted and fixed scaffold implant was a good fit on the left side of the larynx immediately after the operation (Figure 6B), and the implant surface was covered with soft tissues on day 8 after operation (Figure 6C). The surface of the implant was completely proliferated with regenerated mucosal cells 3 weeks (Figure 6D), followed by structural framing of stabilized contours of the regenerated vocal fold without displacements. The bulge of the regenerated vocal fold was still maintained at 20 months after operation.

At 15 months after operation, a CT image (Figure 8) revealed a molded vocal fold, which had a contour structurally resembling the contralateral control larynx without obvious cartilage regeneration.

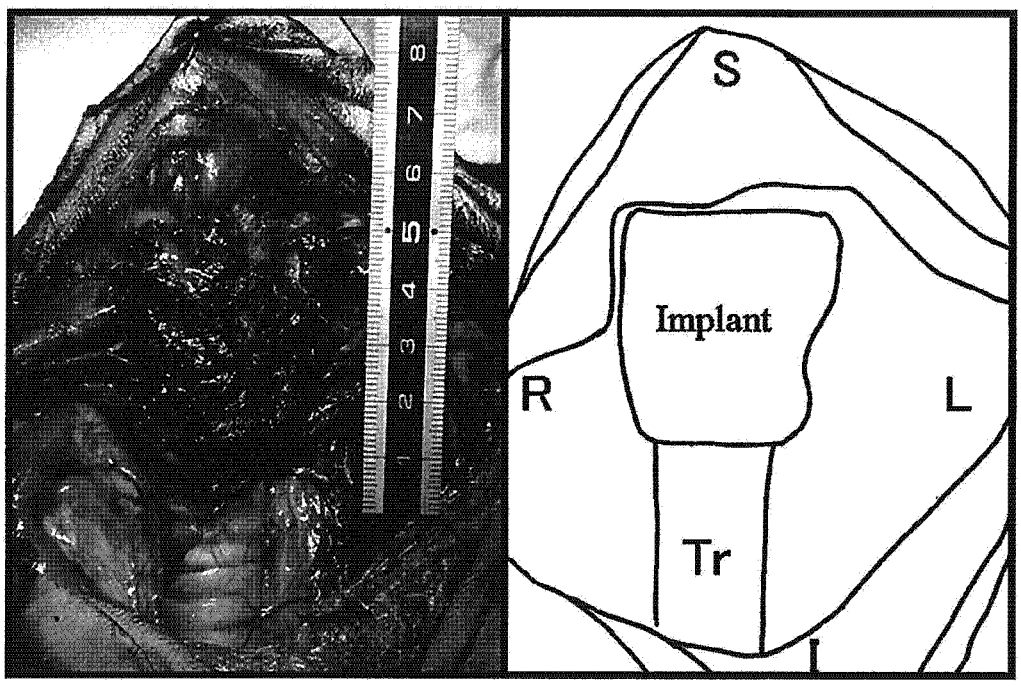

Figure 5. The larynx after implant fixation (left panel) with an illustrative diagram (right panel) for reference. Tr, trachea; S, superior; I, inferior; R, right; L, left.

Table I. Endoscopic findings.

Dog	Stenosis	Epithelialization	Granulation	Exposure of mesh
X	–	Poor	–	+
Y	–	Poor	+	+
Z	–	Good	–	–

Discussion

Various options to reconstruct the larynx after partial surgical resections and/or structural damage have been pursued for more than 50 years [4–11]. However, hitherto established treatments have remained controversial as surgeons continued to encounter inconsistent and incomplete outcomes in laryngeal reconstructions. Factors contributing to unsatisfactory outcomes include: (i) difficulty in reconstructing delicate tissues and structures (having other functions), which are anatomically located in the practically inaccessible larynx, which as a whole is influenced by movements of swallowing and vibrations of vocal cords; (ii) the organ per se is located at an impractically accessible anatomical site; and (iii) factor (i) imposes high-risk operative procedures. Although autologous tissues [4–11] and homografts [12,13] have hitherto been employed as implant materials for laryngeal reconstruction, damage inflicted on the donor site and/or the risk of donor–recipient disease transmissions warrants a more useful and a clinically more efficient approach. Moreover, in cases with tumors in the larynx, deformities of the reconstructed site render it difficult to monitor tumor recurrence. Furthermore, unintentionally inflicted cosmetic handicaps in operated patients sometimes mold unfavorable psychological outcomes that eventually overwhelm the reconstruction effort.

Regenerative medicine has recently been accepted as a useful clinical discipline that ensures and

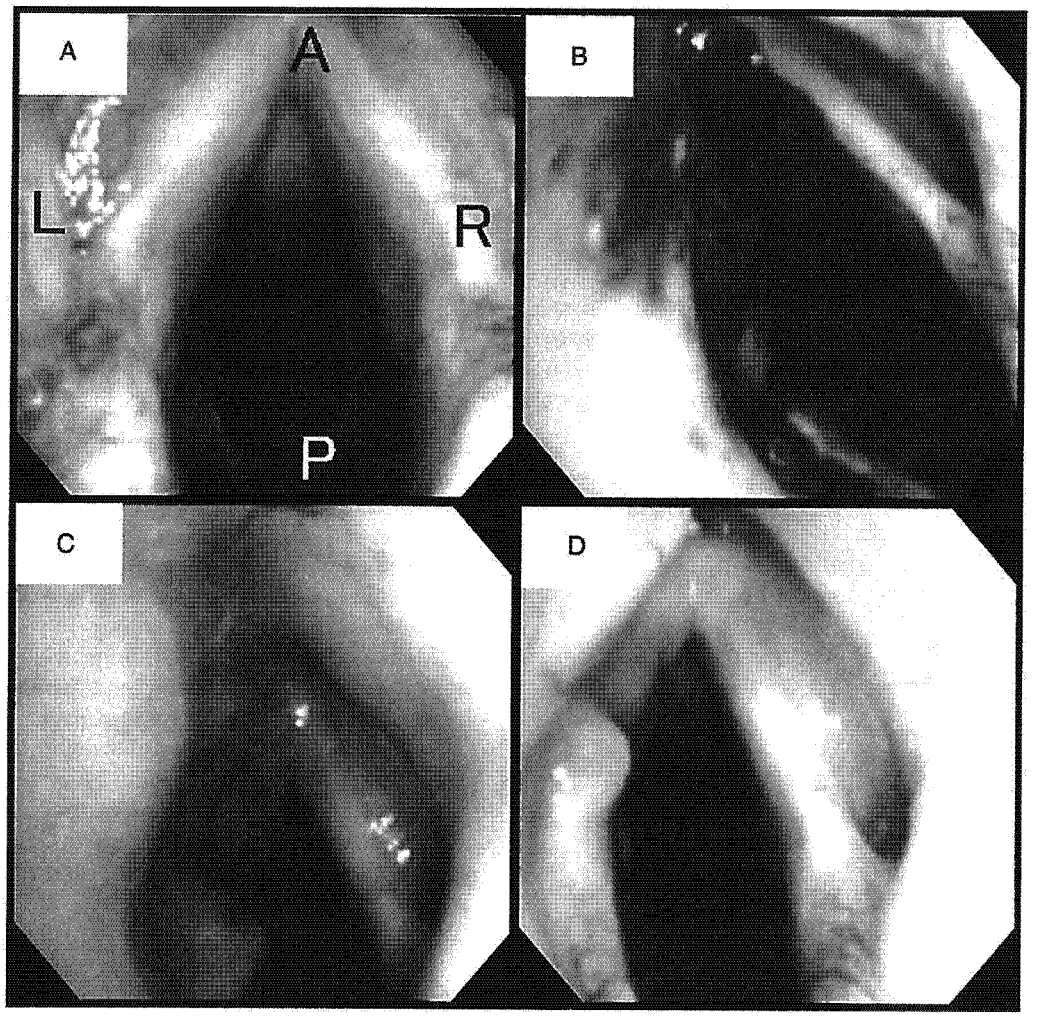

Figure 6. Endoscopic findings of canine case Z before (A), immediately after (B), day 8 (C) and 3 weeks (D) after implantation. A, anterior; P, posterior; R, right; L, left.

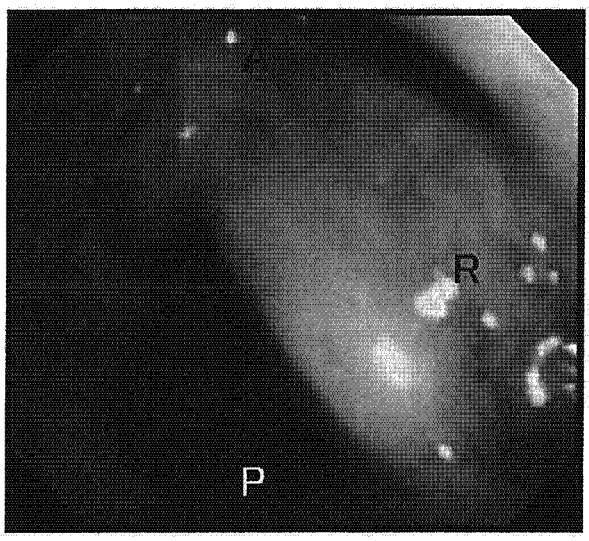

Figure 7. Endoscopic findings of canine case Z at 20 months after operation. A, anterior; P, posterior; R, right; L, left.

enhances the quality of life in patients undergoing organ reconstructions. Improved tissue engineering techniques have facilitated successful regeneration of various organs/tissues. The usual technique exploits three fundamental components: (A) cells acting as 'seeds' for tissue regeneration; (B) a scaffold where cells can proliferate and grow; and (C) regulatory factors which mediate cell behaviors.

A recent concept in in situ tissue engineering, involving the application of a porous microcellular scaffold innovated in vitro for mediating tissue repairs and regeneration processes, was proposed. This concept may allow us to omit component (A) and/or (C), which are available from surrounding tissues of the operated site.

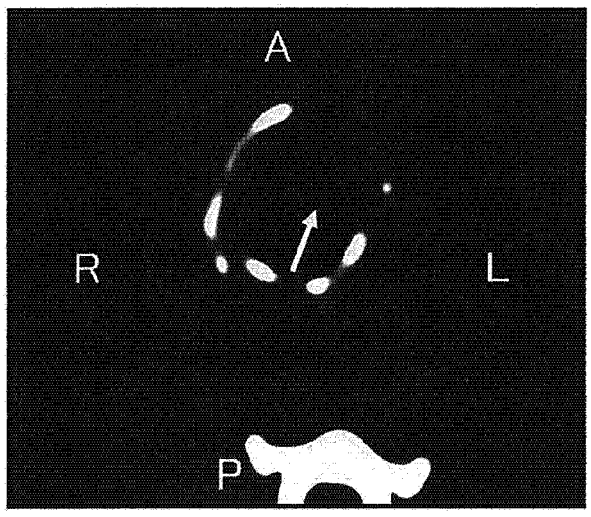

Figure 8. A CT image of canine case Z taken 15 months after implantation. The white arrow shows a bulge of the regenerated implant surface. A, anterior; P, posterior; R, right; L, left.

Our group has achieved useful outcomes in regeneration of the trachea [14,15], esophagus [16], stomach [17], and cricoid area [18] with this in situ tissue engineering technique.

Using tracheal prosthesis with porous-type collagen and polypropylene as a scaffold, Nakamura et al. [14] and Okumura et al. [15] have previously achieved favorable outcomes in canine tracheal regeneration; i.e. favorable cellular invasions of intact collagen, proper epithelialization on the luminal side of implants; and complete integration of the scaffold with the recipient's tissue were established. In addition, Omori et al. [18] have also demonstrated feasible outcomes with scaffolds containing polypropylene with spongy collagen for cricoid regeneration. In the present study, we prepared a novel scaffold using a replication of the luminal shape from a canine larynx to achieve structurally agreeable contours and improved efficacy in laryngeal reconstruction. Since polypropylene is widely used as a polymer with high biocompatibility and feasible morphological adjustability, it was appropriated as the framework material for the present novel scaffold. As polypropylene-treated scaffolds without BSCs produced unfavorable outcomes in our previous experiments, we employed BSCs in the present innovated scaffold.

Although BSCs containing mesenchymal stem cells reportedly differentiate into mesodermal tissues that eventually form muscle, bone, cartilage, etc., recent studies have revealed their potential to differentiate into other lineages such as neural [19] and epithelial tissues/structures [20,21]. The actual contributions of BSCs to the results have not been confirmed yet; however, these cells may have differentiated into epithelial cells and/or secreted certain regenerative factors.

According to Huber et al. [22], favorable outcomes in tissue engineering regeneration of canine larynx after partial hemilaryngectomy can be established with a xenogenic extracellular matrix derived from the acellular urinary bladder.

Functional recoveries with improved phonation, morphological improvement, and histological evaluations are warranted in our approach.

As the outcomes were excellent with the present cost-effective tissue engineering technique and less invasive surgical approach, our novel scaffold and regenerative technique may replace conventional surgical approaches in laryngeal reconstructions.

Conclusions

An experimental model using a scaffold infiltrated with bone marrow-derived stromal cells was innovated for laryngeal regeneration after partial resection